Journal of Applied Polymer Science

# Fabrication and Characterization of the Orientated MMT/PI Composite Films via Relatively Low Magnetic Field

**Fengzhu Lv,[1] Linan Xu,[1] Zixian Xu,[1] Liling Fu,[2] Yihe Zhang[1]**

[1]National Laboratory of Mineral Materials, School of Materials Science and Technology, China University of Geosciences (Beijing), Beijing 100083, China

[2]Department of Materials Science and Engineering, Cornell University, Ithaca, New York 14853

Correspondence to: F. Lv (E-mail: lfz619@cugb.edu.cn) and Y. Zhang (E-mail: zyh@cugb.edu.cn)

**ABSTRACT:** Anisotropic cetylpyridinium modified magnetic montmorillonite/polyimide (CPC-$Fe_3O_4$-MMT/PI) composite films were prepared based on CPC-$Fe_3O_4$-MMT capable of exfoliation and magnetic-field response via *in situ* polymerization and relatively low magnetic field adjustment (0.6 T) in the film casting followed by imidization. The stability of CPC-$Fe_3O_4$-MMT during the *in situ* polymerization over flow shearing of the polymers and longtime stirring was evaluated by comparison the composition of CPC-$Fe_3O_4$-MMT before and after polymerization via TG analysis and element analysis. Besides, the structural anisotropy of the produced CPC-$Fe_3O_4$-MMT/PI composite films deriving from orientation of plate-like CPC-$Fe_3O_4$-MMT was confirmed by 1-D and 2-D XRD and SEM. The CPC-$Fe_3O_4$-MMT/PI composite films with structural anisotropy exhibit gas permeation, optical and magnetic anisotropic properties which would widen the application fields of the composite films. © 2014 Wiley Periodicals, Inc. J. Appl. Polym. Sci. **2015**, *132*, 41224.

**KEYWORDS:** composites; films; magnetism and magnetic properties; optical and photovoltaic applications; polyimides

Received 10 April 2014; accepted 26 June 2014

**DOI: 10.1002/app.41224**

## INTRODUCTION

Recently, extensive research studies have been focused on the development of novel and advanced functional materials by aligning the inorganic nanoparticles in the polymers.[1,2] In contrast to the conventional polymer-based nanocomposites, the aligned nanocomposites possess enhanced optical, mechanical, magnetic, electrical, and thermal properties.[3,4] To properly orient the nanoparticles in a polymeric matrix, several methods have been developed using shear or flow,[5,6] mechanical stretching,[7,8] external electric field,[9–11] and magnetic field.[6,12,13] Among these techniques, alignment of nanoparticles by a magnetic field is an efficient, easy, and wireless one. The magnetic energy acquired by a particle for orientation is to overcome the thermal disturbance (small particles) or the gravity (large particles).[14,15] The resultant materials with aligned particles exhibit potential applications in the fields of biomedicine, magnetic fluid, magnetic recording materials, molecular separation, and electromagnetic wave absorption, and so on.[16] Most current works focus on the alignment of linear[10,17] or spherical nanoparticles[18] since the alignment behavior of the lamellar nanoparticles is complicated and it is difficult to produce nanocomposite materials with an aligned lamellar inorganic structure by magnetic field. Even thought, Liu et al.[3] reported the alignment of disk-shaped iron oxide nanoparticles in the microporous cellulose films derived from the self-orientation of the disk-shaped iron oxide in the shrinkage process of the film at the drying stage. But, it is still a big challenge to successfully align lamellar inorganic particles, especially non-magnetic lamellar materials such as lamellar clay and layered double hydroxides by magnetic field in the polymers.

Montmorillonite (MMT), as a very common lamellar clay, has been widely used to prepare MMT/polymer composites due to its nanolayered structure and plate-like morphology as well as its high aspect ratio.[19] The orientation of MMT in polymer matrices induced by flow-shearing or hot-pressure has been extensively studied.[20–22] The formed composites possess structural anisotropy and exhibit enhanced mechanical properties, dielectric properties, gas barrier properties, and high thermal stabilities. The alignment of MMT by external magnetic field adjustment has rarely been investigated due to the application of a strong applied magnetic field (~2 T).[23] The alignment of organically modified MMT within an epoxy resin at room temperature has been realized by application of static magnetic fields (1.2 or 11.7 T).[24] It is reported that coating diamagnetic

Additional Supporting Information may be found in the online version of this article.

© 2014 Wiley Periodicals, Inc.

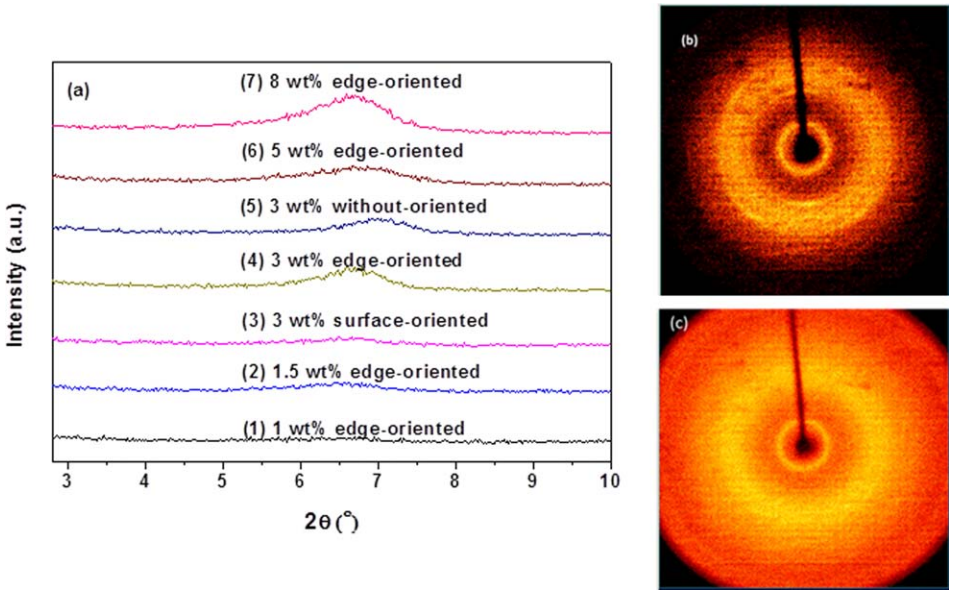


**Figure 1.** 1-D XRD patterns of (a) the CPC-$Fe_3O_4$-MMT/PI composite films with different amounts of CPC-$Fe_3O_4$-MMT prepared in different magnetic fields. The 2-D XRD patterns from (b) the edge-oriented and (c) the surface-oriented CPC-$Fe_3O_4$-MMT/PI composite films. The CPC-$Fe_3O_4$-MMT content of the composition film used here is 3 wt %. [Color figure can be viewed in the online issue, which is available at wileyonlinelibrary.com.]

matters with superparamagnetic nanoparticles will make them more responsive to external magnetic fields. The organic magnetic MMTs (CPC-$Fe_3O_4$-MMT) capable to exfoliate and orient in polymer matrix in a relatively low magnetic field have been developed in our group.[25] In the present work, aligned CPC-$Fe_3O_4$-MMT/PI composite films were prepared in 0.6 T magnetic field. The orientation behaviour of CPC-$Fe_3O_4$-MMT in the matrices of polyimide (PI) and polyamic acid (PAA, precursor of PI) via low magnetic field adjustment was studied. The microstructures, optical properties, gas barrier properties and magnetic anisotropic properties of the produced CPC-$Fe_3O_4$-MMT/PI composite films are characterized by X-ray diffraction (XRD), field emission-scanning electron microscopy (FE-SEM), Ultraviolet and visible light transmission (UV-Vis), and vibrating sample magnetometer (VSM).

## EXPERIMENTAL

### Materials

4,4′-Oxydianiline (ODA) and Pyromellitic anhydride (PMDA) were supplied by Mitsubishi Gas Chemical Company, Japan. Cetylpyridinium chloride (CPC) and *N,N*-dimethylacetamide (DMAc) were purchased from Sinopharm Chemical Reagent, China which was purified by molecular sieves before use. All other chemicals, purchased from Beijing Chemical Reagent Factory, were of analytical grade and used as received without further purification.

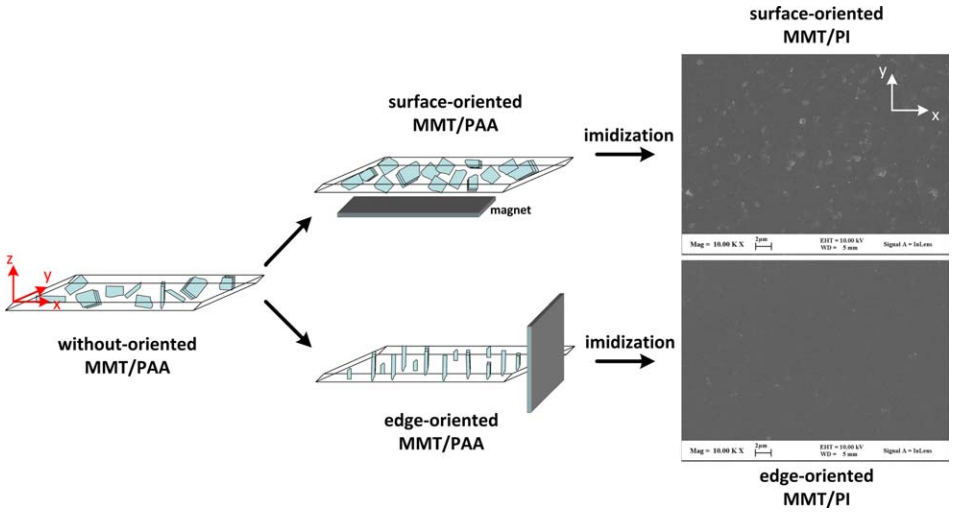


**Scheme 1.** Schematic illustrations of the different orientations of the MMT layers in the composite films. [Color figure can be viewed in the online issue, which is available at wileyonlinelibrary.com.]

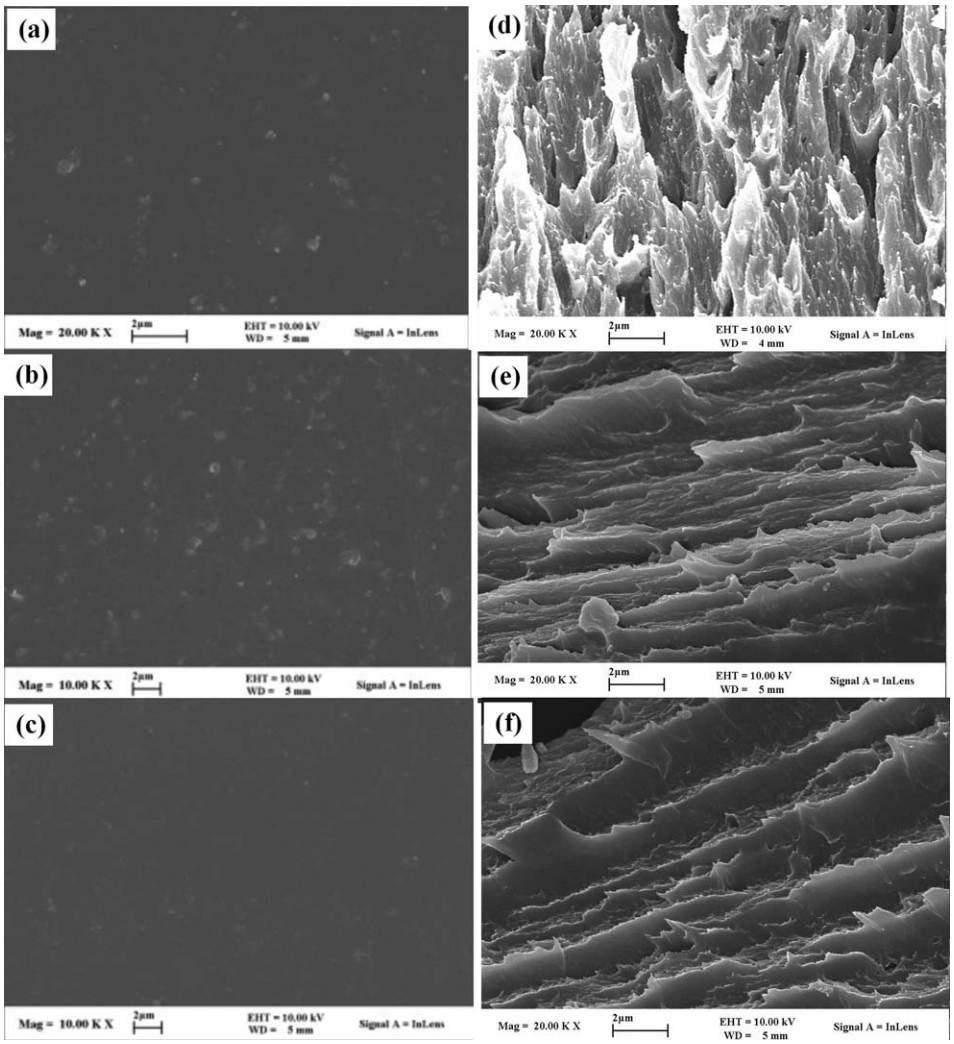


**Figure 2.** Surface SEM images (a–c) and cross-sectional SEM (d–f) of (a, d) non-oriented, (b, e) surface-oriented and (c, f) edge-oriented composite film with 3 wt % of CPC-Fe3O4-MMT.

### Preparation of Anisotropic CPC-$Fe_3O_4$-MMT/PI Composite Films

CPC-$Fe_3O_4$-MMT was prepared based on the method reported on our previous work[25] and the weight ratio of $Fe_3O_4$/MMT used here is 1/14. Briefly, CPC-$Fe_3O_4$-MMT was prepared by first mixing $Fe_3O_4$ and $Na^+$-MMT suspensions with opposite charges in water, followed by further intercalation with CPC in water.

The anisotropic CPC-$Fe_3O_4$-MMT/PI nanocomposite films with a thickness of ~50 μm were prepared by *in situ* polymerization of ODA and PMDA in the presence of CPC-$Fe_3O_4$-MMT and then fabrication of oriented CPC-$Fe_3O_4$-MMT/PAA films in different magnetic fields followed by thermal imidization.[26] In a typical synthesis, 0.129 g of CPC-$Fe_3O_4$-MMT powder was dispersed in DMAc (53.2 mL) and ultrasonicating for 3 h. Then 2.002 g (10.00 mmol) of ODA was dissolved in the CPC-$Fe_3O_4$-MMT suspension with mechanical stirring. After 1 h, 2.214 g (10.15 mmol) of PMDA was added slowly within 1.5 h. A transparent viscous mixture, assigned as CPC-$Fe_3O_4$-MMT/PAA, was formed after stirring for 6 h at 0°C. The obtained mixture was casted on a clean glass slide to form a uniform film and then oriented with a ~0.6 T magnetic field horizontal or perpendicular to the glass slide surface. Then the solid thin film was formed by partial solvent evaporation at 60°C in the external magnetic field and followed by imidization of the thin film. The imidization was performed in a convection oven using the stepwise thermal process: holding the sample in sequence at 80, 100, 130, and 170°C for 30 min and then 200, 250, 300, and 350°C for 1 h, respectively. The obtained composite films (3 wt % of CPC-$Fe_3O_4$-MMT) prepared in the film-surface-parallel and the film-surface-vertical magnetic fields were assigned as the surface-oriented and the edge-oriented CPC-$Fe_3O_4$-MMT/PI films, respectively.

### Instruments for Characterization

The 1-D XRD curves were recorded on a Rigaku D/Max-rA rotating anode X-ray diffractometer equipped with a Cu Kα

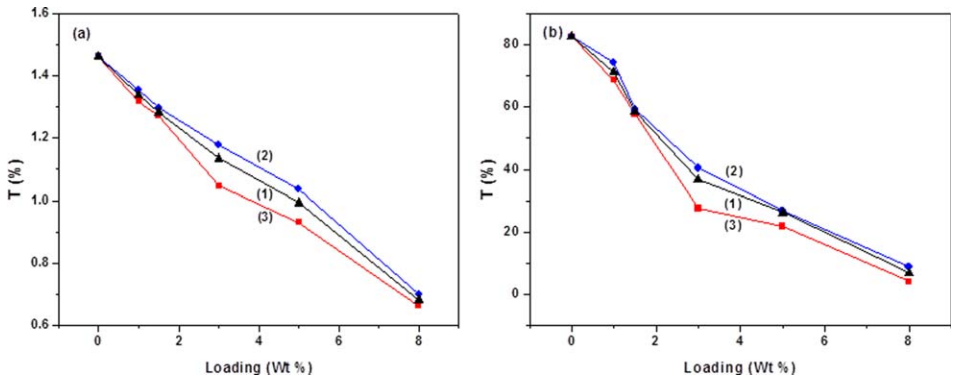


**Figure 3.** UV-Vis transmission of the different orientated 3 wt % CPC-$Fe_3O_4$-MMT/PI composite films at (a) 369 nm and (b) at 600 nm. (1) Non-oriented, (2) edge-oriented, and (3) surface-oriented composite films. [Color figure can be viewed in the online issue, which is available at wileyonlinelibrary.com.]

tube and a Ni filter ($\lambda = 0.15406$ nm). The 2-D XRD patterns were obtained on a Bruker general area detector diffraction system with a HI-STAR area detector. TGA measurements were performed on a TGA Q50 with a heating rate of 10°C/min, scanning from room temperature up to 800°C in $N_2$ stream. The UV-Visible transmission spectra of thin films were measured at room temperature by a UV 765 spectrometer. FE-SEM images were acquired from a LEO-1530 field emission scanning electron microscope operated at 5 kV. The magnetic hysteresis loops were recorded on a PPMS-9T VSM.

Water vapor transmission (WVT) tests were performed on the uniform membranes (~50 $\mu$m of thickness). The membrane was placed at the top of the vial which was pre-filled with distilled water. The humidity of the whole system was maintained at 53% by the saturated aqueous solution of $Mg(NO_3)_2$, while the temperature was set at 27 ± 2°C. The total weight of the vial with membrane was continuously recorded after a period of time.[27]

## RESULTS AND DISCUSSION

### Structural Anisotropy of the CPC-$Fe_3O_4$-MMT/PI Composite Films

Figure 1(a) shows the low angle 1-D XRD patterns of the CPC-$Fe_3O_4$-MMT/PI composite films with different amounts of CPC-$Fe_3O_4$-MMTs prepared in different magnetic fields. The (001) diffraction peak of CPC-$Fe_3O_4$-MMT can be used to character its dispersion in PI matrix. As the (001) diffraction peak of CPC-$Fe_3O_4$-MMT shifts to lower angle, the space of MMT interlayer becomes bigger and the dissociation degree of CPC-$Fe_3O_4$-MMT aggregates is increased. According to Bragg diffraction, crystalline face parallel to the light-normal surface has no contribution to diffraction, so sample with lower diffraction peak possesses more MMT layers which is parallel with the light-normal surface or vertical to the surface of the composite film. In the present work, the (001) diffraction intensity of the composite films increases with the increasing amount of CPC-$Fe_3O_4$-MMT. For example, in a series of the surface-oriented composite films, no diffraction peaks are found when the amount of CPC-$Fe_3O_4$-MMT is less than 3 wt % [Figure 1(a), line 1, 2], which means CPC-$Fe_3O_4$-MMTs are exfoliated fully and dispersed homogeneously in PI matrix.[23] However, the small peaks corresponding to the (001) basal spacing of MMT become obvious with the further increase of CPC-$Fe_3O_4$-MMT [Figure 1(a), line 4, 6, 7] because of the formation of clay tactoids in the samples. In the present work, the change of the (001) diffraction peak of CPC-$Fe_3O_4$-MMT is used to characterize the orientation of MMT layers, so composites with 3 wt % of CPC-$Fe_3O_4$-MMT is oriented in different magnetic fields. The basal peak of all the samples prepared in different directional magnetic fields slightly shifts and its intensity varies due to the different orientations [Figure 1(a), line 3, 4, 5]. The relative intensity of the surface-oriented sample [Figure 1(a), line 4] is larger than that of the non-oriented film [Figure 1(a), line 5] and that of the edge-oriented sample [Figure 1(a), line 3]. Therefore, the samples prepared in film-surface-parallel magnetic field possess the surface-oriented structure due to its relatively high diffraction peak, which means more MMT layers are parallel to the film surface.[28] The appearance of (001) basal spacing plane of the edge-oriented sample, which might not be found if all the MMT layers are vertical to the film surface, confirms that still small proportion of the MMT layers are parallel to the film surface, but the lower (001) diffraction intensity shows that most of MMT layers are perpendicular to the film surface and the samples prepared in film-surface-vertical magnetic field exhibit the edge-oriented structure. The existing states of CPC-$Fe_3O_4$-MMT in the composites prepared in different magnetic field are shown in Scheme 1. Furthermore, compared with the non-oriented films, the (001) peak of the surface-oriented and the edge-oriented films shifts to high angle, which indicates the expansion of the layer spacing in the oriented films. This result also confirms that the magnetic orientation is beneficial for exfoliation.

Generally, 2-D XRD patterns can directly reflect the orientation of the laminated monocrystals and the clay tactoids.[22,23] But as the thickness (~50 μm) of the films prepared in the present work is too thin for 2-D XRD scanning of the fracture surface, therefore only the images of film surfaces are obtained. The 2-D XRD patterns of the edge-oriented [Figure 1(b)] and the surface-oriented [Figure 1(c)] films are almost uniform round cycles due to the contribution of the MMT layers parallel to the film surface. But the contrast of the XRD pattern of edge-

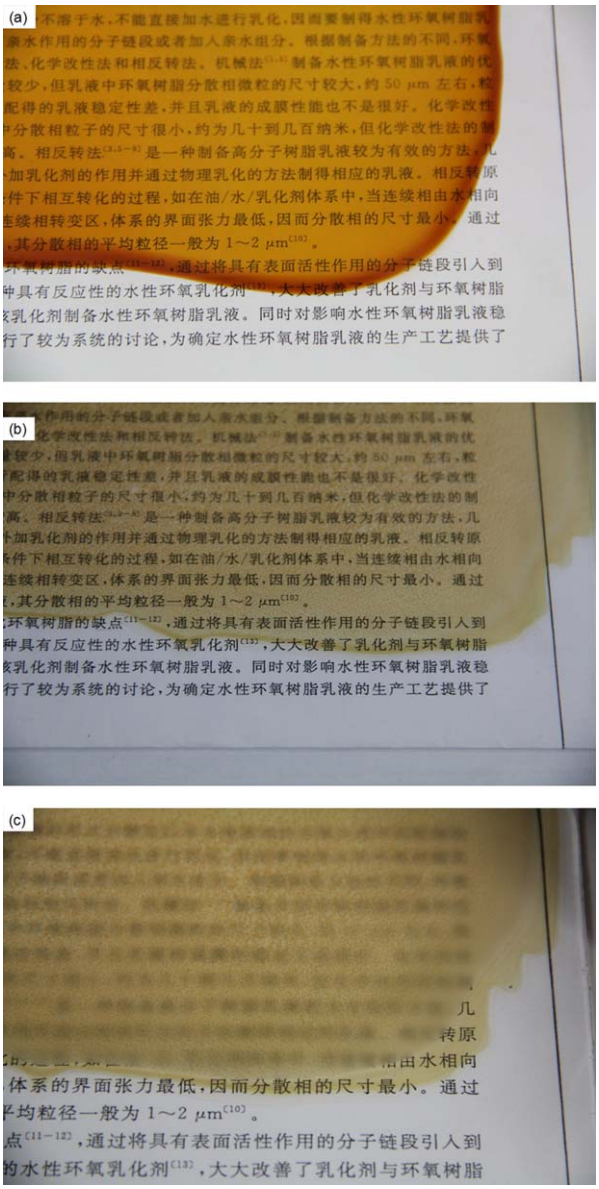


**Figure 4.** Optical properties of (a) the non-oriented CPC-$Fe_3O_4$-MMT/PI and the CPC-$Fe_3O_4$-MMT/PAA composite films in (b) film-surface-vertical, and (c) film-surface parallel magnetic fields. [Color figure can be viewed in the online issue, which is available at wileyonlinelibrary.com.]

oriented film is smaller compared to that of surface-oriented film since most of the MMT layers are vertical to the surface and only small part of the MMT layers are parallel to the film surface. Also the width of the XRD cycle of edge-oriented film is larger with respect to that of surface-oriented film indicating that CPC-$Fe_3O_4$-MMTs with different exfoliation degree coexist in edge-oriented film and CPC-$Fe_3O_4$-MMTs are much easy to exfoliate in vertical magnetic field.

The structural anisotropy is further characterized by SEM and the surface morphologies of the CPC-$Fe_3O_4$-MMT/PI composite films with 3 wt % CPC-$Fe_3O_4$-MMT are displayed in Figure 2. The white spots in Figure 2(a,b,c) represent the CPC-$Fe_3O_4$-MMTs in the polymer matrix. Compared with the non-oriented [Figure 2(a)] and the edge-oriented films [Figure 2(c)], the CPC-$Fe_3O_4$-MMT layers in the surface-oriented films [Figure 2(b)] are easy to be observed and are parallel to the film surface indicating the structural anisotropy of the composite films. In addition, no large aggregates of the MMT layers are observed due to the uniform dispersion of the MMT layers. The cross-sectional SEM morphology of the composites with 3 wt % CPC-$Fe_3O_4$-MMT are also observed. In the cross-sectional image of oriented composites, breaking trace of PI is parallel to each other in one direction [Figure 2(e,f)]. While in the non-oriented composites [Figure 2(d)], the breaking trace is random presenting the orientation of the composites treated under magnetic field.

### Anisotropic Properties of the CPC-$Fe_3O_4$-MMT/PI Films

**Optical Anisotropy.** The UV-Vis transmittance of the CPC-$Fe_3O_4$-MMT/PI composite films is shown in Figure 3. The pure PI exhibits 1.46% of UV transmittance at 369 nm and 82% of visible transmittance at 600 nm. The UV-Vis light transmittances of all the composite films at 369 nm [Figure 3(a)] and 600 nm [Figure 3(b)] decrease with the increase of the CPC-$Fe_3O_4$-MMT content. And the UV transmittance of all the composite films is dramatically lower than that in the visible region, which indicates the higher UV absorption of CPC-$Fe_3O_4$-MMT.[29,30] That is, the addition of clay improves both the UV and visible light shielding, but more in UV light region. Moreover, the orientation of CPC-$Fe_3O_4$-MMT under different directional magnetic field also influences the UV-Vis transmittance of the composite films. With the same loading amount of CPC-$Fe_3O_4$-MMT, the edge-oriented composite films have the highest transmittance [Figure 3(a,b), line 2], and the surface-oriented samples [Figure 3(a,b), line 3] show the lowest one due to the area difference of the MMT layer capable of adsorption of light. The edge-oriented films possess smallest area capable of adsorption of lights as them passing through the film due to most of the MMT layers perpendicular to the film surface. Non orientated PI composite films have randomly dispersed MMT layers in PI matrix, whose influence on transmittance is a collaborative process. Therefore light transmission degree is the middle one [Figure 3(a,b), line 1] among the three sets of samples regardless of the CPC-$Fe_3O_4$-MMT loading.

The visible transmission properties of the anisotropic films is further studied by the transparency of films. Due to the good visible transmission, the words behind the non-oriented composite films with 3 wt % of CPC-$Fe_3O_4$-MMT can be read clearly [Figure 4(a)]. The CPC-$Fe_3O_4$-MMT/PAA films possess adjustable viscosity which is used to avoid the dark red color for clear observation. While film-surface-parallel magnetic field is applied, the clear words behind the CPC-$Fe_3O_4$-MMT/PAA composite films gradually become dim after 30 min because of the light-hinder effect of MMT [Figure 4(c)]. Once the applied magnetic field changes to the film-surface-vertical direction, the unclear words behind the film become clear gradually and back to the original state [Figure 4(b)]. The composite films of CPC-$Fe_3O_4$-MMT/PAA exhibit reversible optical anisotropic properties and the optical responses to the different magnetic directions indicate that the visible transmittance of the edge-oriented composite films is greater than that of the surface-oriented one.

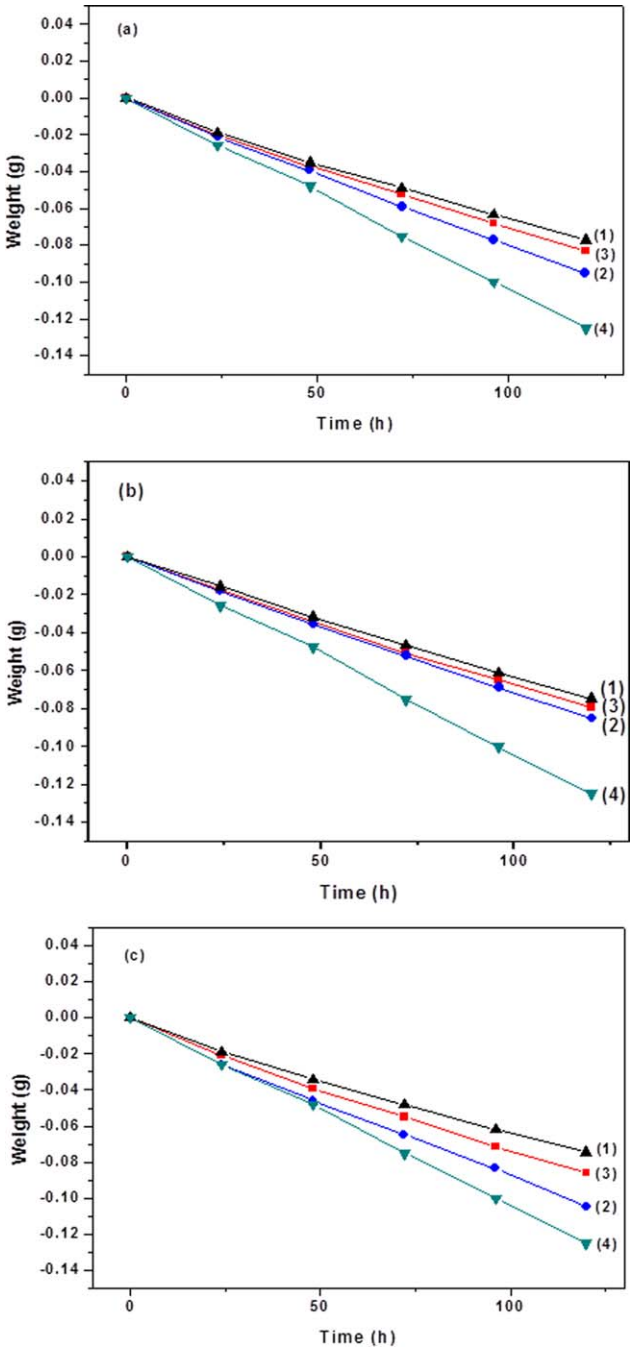


**Figure 5.** Water vapor permeability of (1) the non-oriented, (2) the edge-oriented, (3) the surface-oriented CPC-$Fe_3O_4$-MMT/PI composite films, and (4) the pure PI film. Each sample contains (a) 1 wt %, (b) 3 wt %, and (c) 5 wt % of CPC-$Fe_3O_4$-MMT and is measured at room temperature with 53% of a relative humidity. [Color figure can be viewed in the online issue, which is available at wileyonlinelibrary.com.]

The structural anisotropicy of CPC-$Fe_3O_4$-MMT/PAA are conserved after imidization in different magnetic fields, and the produced CPC-$Fe_3O_4$-MMT/PI composite films have fixed optical anisotropic properties.

**Water Vapor Permeation Anisotropy of the Composite Films.** Figure 5 displays the water vapor permeation of the different orientated composite films. More weight loss of the films covered tube containing water means more water vapor molecules permeation out of the film. The water vapor permeability of the composite films is lower than that of the pure PI film regardless of the orientation of the CPC-$Fe_3O_4$-MMTs, due to the increase of the tortuous paths for water molecules passing through.

In general, the gas permeability of the composite films decreases as the layer matrix is blocked by the layered clays.[28,31,32] The high aspect ratio and the rigid-platelet structure of CPC-$Fe_3O_4$-MMTs force water molecules travelling the film via a tortuous path, thereby increasing the effective path length.[33] The permeability decrease of the composites films regardless of the orientation is in well agreement with the above principle. At fixed inorganic content, the permeability of the non-oriented samples (Figure 5, line 1) is orderly lower than that of the surface-oriented (Figure 5, line 2) and the edge-oriented films (Figure 5, line 3) indicating that water molecules travel a longest distance through the non-oriented samples and a shortest distance through the edge-oriented films. That is, the non-oriented samples possess the most complex paths for vapor diffusion due to the disordered dispersion of CPC-$Fe_3O_4$-MMT. The orientation of CPC-$Fe_3O_4$-MMT in the surface-oriented films results in the greater tortuosity, thereby a more tortuous path is formed for water molecule diffusion compared with that of the edge-oriented films.[23] The different vapor permeability pathways in the various oriented composite films are illustrated in Scheme 1 by arrows. The results also indicate that the alignment of the CPC-$Fe_3O_4$-MMT layers depends on the applied magnetic field, which has been also confirmed by XRD and the optical transmission measurement.

**Magnetic Anisotropy.** Figure 6 shows the magnetization variation with the applied magnetic field at room temperature for the different oriented CPC-$Fe_3O_4$-MMT/PI composite films. All the composite films exhibit a nonobvious hysteresis loop and a small saturated magnetization (*Ms*) regardless of the applied magnetic fields, which indicates the superparamagnetic behaviors of the composite films.[34] As the applied magnetic field is parallel to the film surface [Figure 6(a)], the *Ms* of the edge-oriented film (line 2) is almost equal to that of the non-oriented film (line 1) but lower than that of the surface-oriented film (Line 3). In the present work, CPC-$Fe_3O_4$-MMT possesses *Ms* of 3.07 emu·$g^{-1}$, so the relative small *Ms* of the composites derives from the low content of CPC-$Fe_3O_4$-MMT and its small *Ms*. Since $Fe_3O_4$ with different morphology uniformly disperses on the MMT layer and its size could not change in the preparation process of the composites, so the *Ms* difference is caused by the aggregation degree of CPC-$Fe_3O_4$-MMT. Surface-oriented composites derives from the formation of relative magnetic domains due to the dissociation of the CPC-$Fe_3O_4$-MMT aggregates. Generally, the *Ms* increases with the size decrease of the magnetic particles.[35] Therefore, the relatively high *Ms* of the surface-oriented samples indicated that the dissociation degree of CPC-$Fe_3O_4$-MMT in it is large which means that the distribution of magnetic MMTs in the surface-oriented samples is quite uniform. The *Ms* of the composite films decreases while the direction of the applied magnetic field changes from horizontal to vertical with the film surface [Figure 6(b)]. For example, the *Ms* of the surface-oriented sample

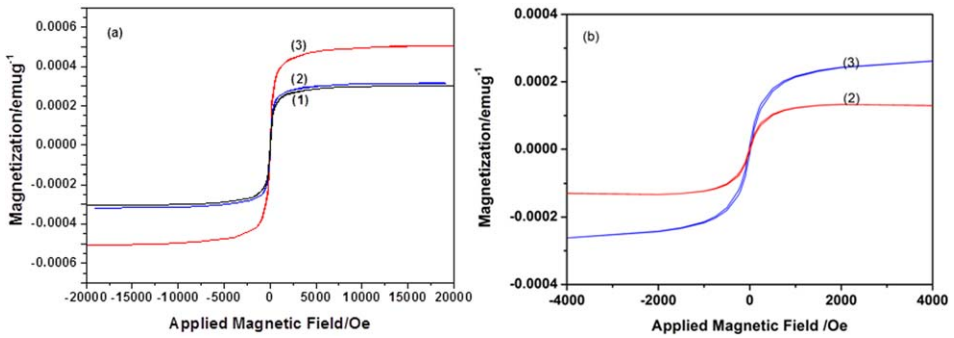


**Figure 6.** Magnetization loops of the CPC-$Fe_3O_4$-MMT/PI composite films with 3 wt % of CPC-$Fe_3O_4$-MMT obtained in (a) the film-surface-parallel and (b) the film-surface-vertical applied magnetic fields. (1) The non-oriented, (2) the edge-oriented, and (3) the surface-oriented composite films. [Color figure can be viewed in the online issue, which is available at wileyonlinelibrary.com.]

decreases from 0.0005 to 0.0003 emu/g. In addition, the magnetic hysteresis loops of the edge-oriented sample from different directions of the applied magnetic fields are displayed in one same Figure (Supporting Information Figure s1). The composite films exhibit different rates to reach the saturated magnetization in different applied magnetic fields indicating the magnetic anisotropy of the composite film.[36]

## CONCLUSIONS

The CPC-$Fe_3O_4$-MMT/PI composite films were prepared by first *in situ* polymerization to provide CPC-$Fe_3O_4$-MMT/PAA precursors and then casting to form films in different magnetic fields followed by imidization. In the process of film casting, the orientation of CPC-$Fe_3O_4$-MMT in PAA was induced by relatively low external magnetic field (0.6 T) and further fixed in the process of imidization. The orientation process not only produces structural anisotropy composite films which is confirmed by 1-D and 2-D XRD as well as SEM, but also improves the exfoliation degree of CPC-$Fe_3O_4$-MMT layers. Thus, the formed composite films have improved anisotropic optical, gas permeation, and magnetic properties which expend the application fields of the composite films, such as reversible switch and magnetic recording film. The surface-oriented composite films have increased *Ms* compared to the edge-oriented composites no matter in film-surface-parallel and film-surface-vertical applied magnetic fields indicating easy magnetization of the edge-oriented composites.

## ACKNOWLEDGMENTS

The work was financially supported by the Fundamental Research Funds for the Central Universities (2-9-2013-49), National Key Laboratory of Minerals (09B003), China, Key Project of Chinese Ministry of Education (107023), Special fund of Co-construction of Beijing Education Committee, and City University of Hong Kong Strategic Research Grant (SRG, 7008009).

## REFERENCES

1. Schmidt, G.; Malwitz, M. M. *Colloid Interface Sci.* **2003**, *8*, 103.
2. Chiu, C. W.; Lin, J. *J. Prog. Polym. Sci.* **2012**, *37*, 406.
3. Liu, S.; Zhou, J.; Zhang, L.; Guan, J.; Wang, J. *Macromol. Rapid Commun.* **2006**, *27*, 2084.
4. Tabatabaei, S. H.; Ajji, A. *Polym. Eng. Sci.* **2011**, *51*, 2151.
5. Okamoto, M.; Nam, P. H.; Maiti, P.; Kotaka, T.; Nakayama, T.; Takada, M.; Ohshima, M., Usuki, A.; Hasegawa, N.; Okamoto, H. *Nano Lett.* **2001**, *1*, 503.
6. Fan, Y.; Lu, Y. C.; Lou, J.; Tang, C. C.; Shinozaki, D. M. *J. Appl. Polym. Sci.* **2013**, *127*, 1387.
7. Jain, A.; Hall, L. M.; Garcia, B. W.; Gruner, S. M.; Wiesner, U. *Macromolecules* **2005**, *38*, 10095.
8. Akima, N.; Iwasa, Y.; Brown, S.; Barbour, A. M.; Cao, J.; Musfeldt, J. L.; Matsui, H.; Toyota, N.; Shiraishi, M.; Shimoda, H.; Zhou, O. *Adv. Mater.* **2006**, *18*, 1166.
9. Martin, C. A.; Sandler, J. K. W.; Windle, A. H.; Schwarz, M. K.; Bauhofer, W.; Schulte, K., Shaffer, M. S. P. *Polymer* **2005**, *46*, 877.
10. Ma, C.; Zhang, W.; Zhu, Y.; Zhang, R.; Koratkar, N.; Liang, *J. Carbon* **2008**, *46*, 706.
11. Huang, Y. P.; Lee, M. J.; Yang, M. K.; Chen, C. W. *Appl. Clay Sci.* **2010**, *49*, 163.
12. Bubenhofer, S. B.; Athanassiou, E. K.; Grass, R. N.; Koehler, F. M.; Rossier, M., Stark, W. *J. Nanotechnology* **2009**, *20*, 485302.
13. Kashem, M. M. A.; Perlich, J.; Diethert, A.; Wang, W.; Memesa, M.; Gutmann, J. S.; Majkova, E.; Capek, I.; Roth, S. V.; Petry, W.; Muller-Buschbaum, P. *Macromolecules* **2009**, *42*, 6202.
14. Kimura, T. *Polym. J.* **2003**, *35*, 823.
15. Erb, R. M.; Libanori, R.; Rothfuchs, N.; Studart, A. R. *Science* **2012**, *335*, 199.
16. Huo, J.; Wang, L.; Yu, H. *J. Mater. Sci.* **2009**, *44*, 3917.
17. Tian, Y.; Park, J. G.; Cheng, Q.; Liang, Z.; Zhang, C.; Wang, B. *Nanotechnology* **2009**, *20*, 335601.
18. Dyab, A. K. F.; Ozmen, M.; Ersoz, M.; Paunov, V. N. *J. Mater. Chem.* **2009**, *19*, 3475.
19. Zhang, Y.; Evans, J. R. G. *Appl. Surf. Sci.* **2012**, *258*, 2098.
20. Dykes, L. M. C.; Torkelson, J. M.; Burghardt, W. R. *Macromolecules* **2012**, *45*, 1622.

21. Pujari, S.; Dougherty, L.; Mobuchon, C.; Carreau, P. J.; Heuzey, M.; Burghardt, W. R. *Rheol. Acta* **2011**, *50*, 3.

22. Nawani, P.; Burger, C.; Rong, L.; Chu, B.; Hsiao, B. S.; Tsou, A. H.; Weng, W. *Polymer* **2010**, *51*, 5255.

23. Uyeda, C.; Takeuchi, T.; Yamagishi, A.; Date, M. *Phys. B* **1992**, *177*, 519.

24. Koerner, H.; Turgut, Z. *Chem. Mater.* **2005**, *17*, 1990.

25. Xu, Z.; Lv, F.; Zhang, Y.; Fu, L. *Chem. Eng. J.* **2013**, *215–216*, 755.

26. Zhang, Y.; Wu, J.; Fu, S.; Yang, S.; Li, Y.; Fan, L.; Li, R.; Li, L.; Yan, Q. *Polymer* **2004**, *45*, 7579.

27. Hayrapetyan, S.; Kelarakis, A.; Estevez, L.; Lin, Q.; Dana, K.; Chung, Y.; Giannelis, E. P. *Polymer* **2012**, *53*, 422.

28. Yuan, G.; Li, X.; Dong, Z.; Westwood, A.; Cui, Z.; Cong, Y.; Du, H.; Kang, F. *Carbon* **2012**, *50*, 175.

29. Mbey, J. A.; Hoppe, S.; Thomas, F. *Carbohydr. Polym.* **2012**, *88*, 213.

30. Wu, T.; Xie, T.; Yang, G. *J. Polym. Sci. Part B Polym. Phys.* **2009**, *47*, 903.

31. Picard, E.; Espuche, E.; Fulchiron, R. *Appl. Clay Sci.* **2011**, *53*, 58.

32. Yano, K.; Usuki, A.; Okada, A. *J. Polym. Sci. Part A Polym. Chem.* **1997**, *35*, 2289.

33. Park, H. M.; Lee, W. K.; Park, C. Y.; Cho, W. J.; Ha, C. S. *J. Mater. Sci.* **2003**, *38*, 909.

34. Fan, L.; Luo, Y.; Chen, Y.; Zhang, C.; Wei, Q. *J. Nanopart. Res.* **2009**, *11*, 449.

35. Atif, M.; Hasanain, S. K.; Nadeem, M. *Solid State Commun.* **2006**, *138*, 416.

36. Yan, L.; Yang, Y.; Wang, Z.; Xing, Z.; Li, J.; Viehl, D. *J. Mater. Sci.* **2009**, *44*, 5080.